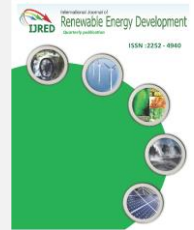




Contents list available at IJRED website


**International Journal of Renewable Energy Development**

Journal homepage: <https://ijred.undip.ac.id>



Research Article

# Offering strategy of a price-maker virtual power plant in the day-ahead market

Nhung Nguyen-Hong<sup>\*</sup> , Khai Bui Quang, Long Phan Vo Thanh, Duc Bui Huynh

*Department of Electrical Engineering, School of Electrical and Electronics Engineering, Hanoi University of Science and Technology, Hanoi, Vietnam*

**Abstract.** With the rapid increase of renewable energy sources (RESs), the virtual power plant model (VPP) has been developed to integrate RESs, energy storage systems (ESSs), and local customers to overcome the RESs' disadvantages. When the VPP's capacity is large enough, it can participate in the electricity market as a price-maker instead of a price-taker to obtain a higher profit. This study proposes a bi-level optimization model to determine the optimal trading strategies of a price-maker VPP in the day-ahead (DA) market. The operation schedule of the components in the VPP is also optimized to achieve the highest profit for the VPP. In the bi-level optimization problem, the upper-level model is maximizing the VPP's profit while the lower-level model is the DA market-clearing problem. The bi-level optimization problem is formulated as a Mathematical Problem with Equilibrium Constraints (MPEC), reformulated to a Mixed Integer Linear Problem (MILP), then solved by GAMS and CPLEX. This study applies the bi-level optimization model to a test VPP system, including wind plants (WP), solar plants (PV), biogas energy plants (BG), ESSs, and several customers. The maximum power outputs of WP and PV are 100MW and 90MW, respectively. The total installed capacity of BG is 70MW, while the ESS' rated capacity is 100MWh. The local customers have the highest total consumption of 100MW. In addition to the VPP, four GENCOs and three retailers participate in the DA market. The results show that the market-clearing price varies depending on the participants' production/consumption quantity and offering/bidding price. However, based on the optimization model, the VPP can take full advantage of WP and PV available power output, choose the right time to operate BG, then obtain the highest profit. The results also show that with the ESS' rated capacity of 100MWh, the ESS' rated discharging/charging power increased from 10MW to 50MW will increase VPP's profit from 45987\$ to 49464\$. The obtained results show that the proposed model has practical significance.

**Keywords:** Day-ahead market, mathematical problem with equilibrium constraints, mixed-integer linear programming, price-maker, renewable energy, virtual power plants.



@ The author(s). Published by CBIORE. This is an open access article under the CC BY-SA license (<http://creativecommons.org/licenses/by-sa/4.0/>).

Received: 22<sup>nd</sup> March 2023; Revised: 2<sup>nd</sup> May 2023; Accepted: 19<sup>th</sup> May 2023; Available online: 27<sup>th</sup> May 2023

## 1. Introduction

In recent years, the penetration level of renewable energy sources (RES), such as wind and solar power, into the power system has rapidly increased. These energy sources satisfy the ever-increasing electricity demand and reduce the use of fossil fuel sources and greenhouse gas emissions. Therefore, governments have launched attractive policies to promote investment in RES, such as allowing RESs to participate in the competitive electricity market. However, due to the difficulties in the power system's operation, most electricity markets require a minimum size of all participants. In some markets, this minimum threshold may be quite small; such as PJM or AESO only requires a tiny threshold of 100kW (Helman, 2019; Neme *et al.*, 2014; Oureilidis *et al.*, 2020). In contrast, some markets require this value to be much higher; for example, in Vietnam, RESs must have an installed capacity of at least 30MW to participate in the electricity market (Electricity Regulatory Authority of Vietnam, 2018). This not only makes small-scale sources not fully exploited but also reduces the interest of investors.

To solve these above problems, the concept of a Virtual Power Plant (VPP) has been developed and gradually become

popular over the past decade. This model can integrate various small-scale RESs, flexible loads, energy storage systems (ESS), and retailers and represents them to enter the wholesale market. The VPP model has been and is being put into practice in Europe and Australia, and the obtained results have shown the effectiveness of this model (AEMO, 2021; Kuiper, 2022; Next-Kraftwerke, n.d.). The reports (AEMO, 2021; ARENA, 2021) show that VPPs in Australia mainly include solar farms, batteries, and residential customers. By contrast, the inner resources of Next-Kraftwerke's VPP are more diverse with wind farms, solar farms, batteries, and biogas power plants (Next-Kraftwerke, n.d.). Until now, Next-Kraftwerke's VPP includes about 15,000 medium- and small-scale producers and consumers. Meanwhile, AEMO reports that almost 168MW of residential batteries were registered to VPP in June 2021. These reports show the potential of VPP in the future.

According to (Kieny *et al.*, 2009; Pudjianto *et al.*, 2007), there are two types of VPP: Technical VPP (Technical – TVPP) and Commercial VPP (Commercial – CVPP). While the CVPP model only pays attention to profit maximization and ignores the network constraint, the TVPP considers the grid structure and operating standards, such as the voltage at the bus as well as

<sup>\*</sup> Corresponding author

Email: [nhung.nguyenhong1@hust.edu.vn](mailto:nhung.nguyenhong1@hust.edu.vn) (N.Nguyen-Hong)

transmission line capacity. However, both models have an exciting research direction: determining the operating plan for optimal coordination among members in the VPP, also called VPP's self-scheduling problem, thereby achieving maximum profit.

In the literature, many studies have considered VPP as a price-taker that should predict the day-ahead (DA) price as well as the demand/available power output of each customer/resource belonging to VPP (Nguyen *et al.*, 2018; Pal *et al.*, 2021; Yazdaninejad *et al.*, 2020; Zhou *et al.*, 2019). Based on these forecasted data, the VPP operator determines the amount of buying/selling energy each hour on the next day and submits its trading strategy to the market. Also, the operation between flexible loads, RES, or ESSs is coordinated to take advantage of RES's available power output and compensate for forecasting errors. In (Baringo & Baringo, 2017; Pal *et al.*, 2021; Yazdaninejad *et al.*, 2020; Zhao *et al.*, 2016), the authors only consider the VPP's optimal scheduling in the energy market. In (Lee & Won, 2021), the VPP operator should determine the VPP's optimal schedule based on predicted prices of both DA and real-time (RT) markets. In (Nguyen *et al.*, 2018), the VPP can buy demand response service from the intraday demand response exchange (DRX) market to ensure the selling/buying power as the offering/bidding strategy submitted to the day-ahead (DA) market in case the inner resources are insufficient. Besides, in some other studies, VPP not only participates energy market but also provides ancillary services such as spinning reserve (Baringo *et al.*, 2019; Fernández-Muñoz & Pérez-Díaz, 2023; Mashhour & Moghaddas-Tafreshi, 2011; Nguyen-Duc & Nguyen-Hong, 2020; Vahedipour-Dahraie *et al.*, 2021; Zhou *et al.*, 2019). However, regardless of which markets the VPP participates in, the VPP cannot influence the market-clearing price.

Meanwhile, based on advanced information and communication technology and control systems, VPP can fully integrate, manage and operate many resources regardless of geographical location. As a result, VPPs can have a large enough capacity to influence cleared prices, thereby being able to participate in the wholesale electricity market as price-makers. In this case, VPP can increase the overall profit by devising different trading strategies to change the market price. In (Ding *et al.*, 2017), an operational strategy of a price-maker wind farm – energy storage systems in the DA offering and RT operation is proposed to maximize its profit. In (Hu *et al.*, 2019; Kardakos *et al.*, 2016), the VPP operator determines the VPP optimal offering strategy to maximize the VPP's profit in the DA market and minimize the imbalance penalty fee in the RT operation. In (Baringo *et al.*, 2021; Yi *et al.*, 2021), the price-maker VPP joins the energy and reserve market while the DA and RT markets are considered in (Gazijahani & Salehi, 2020). In these articles, the authors propose a bi-level optimization model that includes the upper-level problem of maximizing the VPP's profit and the lower-level problem of determining the market-clearing price. However, it can be seen that there are not many articles focusing on the price-maker VPP model. Not only that, but the current studies also do not pay much attention to biogas power plants, while the potential of biogas power plants in practice is very high. In (Gazijahani & Salehi, 2020), a combined heat and power (CHP) unit is considered; however, the authors focus on only the power part. By contrast, studies (Tavakoli *et al.*, 2021; Yang *et al.*, 2023) take the chemical process to produce biogas fuel into account the optimization problem. Using such a complex model may not be necessary from the viewpoint of the VPP's operator.

Vietnam is a tropical country with a geographical position north of the equator and a long coastline, so Vietnam has abundant potential for both solar and wind energy. The

Vietnamese government also has many policies to help promote the development of these energy sources. According to reports (British Chamber of Commerce Vietnam, 2022; Das, 2020), it is estimated that by 2030, Vietnam can reach 18.6GW of solar and 18GW of wind capacity. Also, the potential for electricity production from biogas is great in Vietnam. Reports (Internationale Klimaschutzinitiative, 2022; Noi *et al.*, 2022) show Vietnam's biogas power capacity can reach 1,400 MW by 2035. Similar to many other power systems worldwide, integrating RESs into the system also causes many challenges due to the uncertainty in RES affecting the power system stability. To solve this problem, the national load dispatch center had to curtail at least 1.3 billion kWh of RES per year to ensure the safety of the power system (Ngo, 2021). Consequently, the profit of RES owners is still reduced despite being allowed to sell electricity at a preferential price. Therefore, developing VPPs to solve the disadvantages of an individual RES operation and increase profit opportunities in a competitive market will become inevitable in Vietnam. However, until now, studies on the VPP model, especially price-maker VPP, are still scarce in Vietnam.

Hence, in this paper, the authors present a bi-level optimization model to obtain VPP's optimal trading strategy in DA as a price-maker. This VPP is assumed to include wind power plants (WP), solar power plants (PV), biogas power plants (BG), large customers, and ESS, in which the operating schedules of these inner resources are also optimally coordinated to utilize their available power output fully. In this paper, the biogas power plant is modeled as a biogas storage and electrical power plant. The flow of gas into the storage each hour is also considered. In the bi-level problem, the upper-level model optimizes the VPP's profit while the lower-level model simulates the DA market clearing process. This problem is formulated as a Mathematical Problem with Equilibrium Constraints (MPEC). By linearization methods proposed by (Steven A. Gabriel *et al.*, 2013), this problem is turned into a Mixed Integer Linear Problem (MILP) and solved by GAMS and CPLEX. The impact of ESS sizing as well as VPP offering/bidding price on the VPP's optimal schedule are analyzed. The rest of the paper is organized as follows: Section 2 demonstrates the optimal scheduling model of a price-maker VPP in the DA market. Section 3 presents the case study, then summarizes and analyzes the results. Finally, Section 4 concludes the paper. The linearization process from MPEC to MILP model is presented in Appendix.

## 2. Problem Description

This paper considers a CVPP model including WP, PV, BG, ESS and demand, as shown in Fig. 1. This is a typical VPP model that has been applied in practice (AEMO, 2021; Kuiper, 2022; Next-Kraftwerke, n.d.). The VPP can act as a supplier or a consumer in the DA market, depending on the difference between RESs' available power output and local demand. ESS accumulates energy if the RESs power output is surplus and the market price is low. By contrast, ESS discharges energy if the RESs cannot satisfy the local demand or the market price is high. In addition, the forecasting error of RES and the customer can also be compensated by ESS' charge/discharge operation. Hence, VPP can ensure its trading schedule in the DA market regardless of inner resources' uncertainty.

In this paper, the VPP is assumed to have a large enough production/consumption to affect the market clearing price. Therefore, the VPP can participate in the DA market as a price-maker. From the VPP operator standpoint, a bi-level optimization problem is proposed to determine the market-

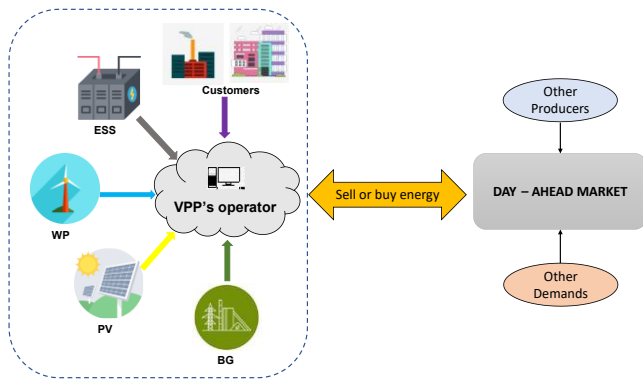


Fig. 1 The VPP's structure

clearing price and the VPP's buying/selling energy at each hour while maximizing the VPP's profit. The upper-level presents the VPP profit maximization, while the lower-level presents the DA market-clearing process. The impact of the VPP's trading strategy on the market-clearing price is formulated by the price quota curves of VPP each hour. Because most of VPP's power sources are RES with very low production costs, the influence of VPP on market prices becomes even more pronounced. It can be seen that the market price is reduced if VPP offers all RESs available power output with an offering price close to the production cost. By contrast, the market price becomes high if RESs in VPP cannot operate.

The below section provides the formulation of the trading strategy of a price-maker VPP participating in the DA market.

2.1 Upper-level problem: The VPP's trading strategy

2.1.1 Objective function

This problem is proposed to maximize VPP's overall profit with the objective function including three major parts as follows:

$$\max F_1 = \lambda_t^E (p_t^{E+} \Delta t - p_t^{E-} \Delta t) - (C^{WD} + C^{BG}) \quad (1)$$

In equation (1), the first term  $\lambda_t^E (p_t^{E+} \Delta t - p_t^{E-} \Delta t)$  defines the VPP's revenue obtained from the DA market. The second term  $C^{WD} = c^{WD} \times p_t^{WD}$  is the WP's operating cost while the third term  $C^{BG} = \sum_i C_i^F \bar{P}_i^B u_{it}^B + C_i^Y p_{it}^B$  is the BG's operating costs that consist of two components, fixed costs and variable costs (Renewable Energy Agency, 2012).

2.1.2 Constraints

The upper-level problem is accomplished under a set of technical constraints describing the offering/bidding between the VPP and DA market.

- Power balance in VPP:

Equation (2) shows that the VPP's buying/selling power in the DA market must be balanced with the production/consumption of the inner resources/customers.

$$p_t^{WD} + p_t^{PV} + p_t^B + p_t^{S,D} = P_{d,t}^{VPP} + p_t^{S,C} + p_t^{E+} - p_t^{E-} \quad (2)$$

- Constraint of VPP offering/bidding strategy in the DA market

Equations (3) and (4) show that the limitation of the VPP offering/bidding power quantity during each hour. These

constraints also keeps that the VPP can only buy or sell electricity to the power system at any time. Equation (5) restricts the VPP's offering/bidding price in the DA market

$$\begin{cases} 0 \leq \bar{P}_t^{E+} \leq u_t^{VPP} (\bar{P}_t^{WD} + \bar{P}_t^{PV} - P_{d,t}^{VPP} + \bar{P}^{BG} + \bar{P}^{S,D}) \\ 0 \leq p_t^{E+} \leq \bar{P}_t^{E+} \end{cases} \quad (3)$$

$$\begin{cases} 0 \leq \bar{P}_t^{E-} \leq (1 - u_t^{VPP}) (P_{d,t}^{VPP} + \bar{P}^{S,C}) \\ 0 \leq p_t^{E-} \leq \bar{P}_t^{E-} \end{cases} \quad (4)$$

$$v_t^{E+}, v_t^{E-} \geq 0 \quad (5)$$

- WP operating constraints:

This constraint shows that the given forecasted available wind power  $\bar{P}_t^{WD}$  and the minimum power threshold  $\underline{P}^{WD}$  limit the WG's power output. This model assumes that the WP cannot be forced to stop.

$$\underline{P}^{WD} \leq p_t^{WD} \leq \bar{P}_t^{WD} \quad (6)$$

- PV operating constraints

Similar to the WP, the power output of the PV be limited by the forecasted available power  $\bar{P}_t^{PV}$ . The binary variable  $u_t^{PV}$  in equation (7) shows that the PV can be decommissioned. This issue will affect the price quota curves of VPP.

$$0 \leq p_t^{PV} \leq u_t^{PV} \bar{P}_t^{PV} \quad (7)$$

- BG operating constraints

Equation (8) shows that the BG power output must be in the operating range between the minimum threshold  $\underline{P}_i^B$  and the maximum threshold  $\bar{P}_i^B$ . The binary variable  $u_{it}^B$  keeps the BG power output equal to zero if it is shut down.

$$u_{it}^B \underline{P}_i^B \leq p_{it}^B \leq u_{it}^B \bar{P}_i^B \quad (8)$$

Each biogas plant has a storage of gas that is input fuel for the plant's electricity production. Assuming that there is a flow of gas  $F_t$  (expressed in MWh) into this storage. Equation (9) defines the change of storage level  $soc_t^B$  (expressed in MWh) after hour  $t$  based on the gas quantity  $F_t$  and the electrical energy generated during each hour. Besides, equation (10) also imposes that the storage level at any time should be smaller than storage capacity  $\overline{soc}_t^B$ .

$$soc_t^B = soc_{t-1}^B + F_t - p_t^B \times \Delta t \quad (9)$$

$$0 \leq soc_t^B \leq \overline{soc}_t^B \quad (10)$$

- ESS operating constraints

Equation (11) describes the ESS charging/discharging process during each hour. Equation (12) shows that the energy level in the ESS must be set to a certain level after each operating day. Besides, equation (13) also shows that the ESS energy level is limited by the minimum and maximum energy level to ensure ESS' lifetime. Equations (14) and (15) show that the charging or discharging power of the ESS should be smaller

than the rated power. The binary variable  $u_t^S$  makes sure that ESS can only operate in charge or discharge mode at any time.

$$e_t^S = e_{(t-1)}^S + \eta^S P_t^{S,C} \Delta t - \frac{P_t^{S,D} \Delta t}{\eta^S} \quad (11)$$

$$e_{24}^S = e_0^S \quad (12)$$

$$\underline{E}_t^S \leq e_t^S \leq \overline{E}_t^S \quad (13)$$

$$0 \leq p_t^{S,D} \leq u_t^S \overline{P}^S \quad (14)$$

$$0 \leq p_t^{S,C} \leq (1 - u_t^S) \overline{P}^S \quad (15)$$

### 2.2 Lower-level problem: Day-ahead market clearing process

#### 2.2.1 Objective function

This problem describes the market-clearing process in the DA market from the power market operator's standpoint, so the objective function is minimizing the minus social welfare as follows:

$$\min F_2 = v_t^{E+} p_t^{E+} + \sum_{g \in \Omega^G} \alpha_{gt}^{G,E} p_{gt}^{G,E} - v_t^{E-} p_t^{E-} - \sum_{q \in \Omega^Q} \alpha_{qt}^{Q,E} p_{qt}^{Q,E} \quad (16)$$

In equation (16), the first two terms,  $v_t^{E+} p_t^{E+}$  and  $\sum_{g \in \Omega^G} \alpha_{gt}^{G,E} p_{gt}^{G,E}$ , are the revenues of the VPP and other producers participating in the DA market, respectively. The remaining two term,  $v_t^{E-} p_t^{E-}$  and  $\sum_{q \in \Omega^Q} \alpha_{qt}^{Q,E} p_{qt}^{Q,E}$ , are the purchasing costs of the VPP and other demand.

#### 2.2.2 Constraints

The lower-level problems is characterized be the following constraints

- The power balance constraint

Equation (17) guarantees that the selling and purchasing power in the DA market will be matched, thereby ensuring the power balance.

$$p_t^{E+} + \sum_{g \in \Omega^G} p_{gt}^{G,E} = p_t^{E-} + \sum_{q \in \Omega^Q} p_{qt}^{Q,E} : \lambda_t^E \quad (17)$$

- Constraint of each producer/customers in the DA market

Equations (18) and (19) show the limitation of VPP's selling/purchasing power in the DA market. Meanwhile, equations (20) and (21) limit the trading power of producers and customers, respectively.

$$0 \leq p_t^{E+} \leq \overline{P}_t^{E+} : \underline{\mu}_t^{E+}, \overline{\mu}_t^{E+} \quad (18)$$

$$0 \leq p_t^{E-} \leq \overline{P}_t^{E-} : \underline{\mu}_t^{E-}, \overline{\mu}_t^{E-} \quad (19)$$

$$0 \leq p_{gt}^{G,E} \leq \overline{P}_{gt}^{G,E} : \underline{\mu}_{gt}^{G,E}, \overline{\mu}_{gt}^{G,E} \quad (20)$$

$$0 \leq p_{qt}^{Q,E} \leq \overline{P}_{qt}^{Q,E} : \underline{\mu}_{qt}^{Q,E}, \overline{\mu}_{qt}^{Q,E} \quad (21)$$

The dual variables in each constraint is declared after a colon, in which the dual variable of the power balance constraint is the DA market-clearing price. Besides, notice that the VPP

offering/bidding price should be determined in the upper-level problem so that in the lower-level problem, these values are treated as input parameters

### 2.3 MILP model

To simplify the presented bi-level problems, the lower-order problem, i.e., the DA market-clearing problem, can be replaced by its Karush-Kuhn-Tucker (KKT) conditions. The transformation is possible because the lower-level problem (16) is convex and linear over its decision variables. Using the transformation approach in (Steven A. Gabriel et al., 2013), we obtain a single-level MPEC problem shown in Appendix. This model comprises primal and dual constraints as well as complementarity slackness conditions corresponding to the inequalities of the original model. It can be seen that the single-level MPEC model contains two nonlinear components: the term  $\lambda_t^E (p_t^{E+} \Delta t - p_t^{E-} \Delta t)$  in the objective function of the upper-level problem; and the complementarity slackness conditions. Applying the linearization method provided by (Steven A. Gabriel et al., 2013), the single-level MPEC model is converted to the following MILP model. The processes of transformation and linearization are presented in Appendix.

$$\max \sum_{t \in \Omega^T} \left\{ \left( \sum_{q \in \Omega^Q} \alpha_{qt}^{Q,E} p_{qt}^{Q,E} - \sum_{g \in \Omega^G} \overline{P}_{gt}^{G,E} \overline{\mu}_{gt}^{G,E} - \sum_{g \in \Omega^G} \alpha_{gt}^{G,E} p_{gt}^{G,E} - \sum_{q \in \Omega^Q} \overline{P}_{qt}^{Q,E} \overline{\mu}_{qt}^{Q,E} \right) - (c^{WD} \times p_t^{WD} + C_i^F \overline{P}_i u_{it} + C_i^V p_{it}^B) \right\} \quad (22)$$

Subject to:

$$p_t^{WD} + p_t^{PV} + p_t^B + p_t^{S,D} = P_{d,t}^{VPP} + p_t^{S,C} + p_t^{E+} - p_t^{E-} \quad (23)$$

$$N \leq p_t^{WD} \leq \overline{P}_t^{WD} \quad (24)$$

$$0 \leq p_t^{PV} \leq u_t^{PV} \overline{P}_t^{PV} \quad (25)$$

$$0 \leq p_{it}^B \leq u_{it}^B \overline{P}_i^B \quad (26)$$

$$soc_t^B = soc_{t-1}^B + F_t - p_t^B \times \Delta t \quad (27)$$

$$0 \leq soc_t^B \leq \overline{soc}_t^B \quad (28)$$

$$e_t^S = e_{(t-1)}^S + \eta^{S,C} P_t^{S,C} \Delta t - \frac{P_t^{S,D} \Delta t}{\eta^{S,D}} \quad (29)$$

$$e_{24}^S = e_0^S \quad (30)$$

$$\underline{E}_t^S \leq e_t^S \leq \overline{E}_t^S \quad (31)$$

$$0 \leq p_t^{S,D} \leq u_t^S \overline{P}^{S,D} \quad (32)$$

$$0 \leq p_t^{S,C} \leq (1 - u_t^S) \overline{P}^{S,C} \quad (33)$$

$$\overline{P}_t^{E+} \leq (\overline{P}_t^{WD} + \overline{P}_t^{PV} - P_d^{VPP} + \overline{P}^B + \overline{P}^{S,D}) u_t^{VPP} \quad (34)$$

$$\overline{P}_t^{E-} \leq (P_d^{VPP} + \overline{P}^{S,C}) (1 - u_t^{VPP}) \quad (35)$$

$$\overline{P}_t^{E+}, \overline{P}_t^{E-} \geq 0 \quad (36)$$

$$v_t^{E+}, v_t^{E-} \geq 0 \quad (37)$$

$$u_t^{PV}, u_{it}^B, u_t^S, u_t^{VPP} \in \{0,1\} \quad (38)$$

$$p_t^{E-} + \sum_{q \in \Omega^Q} p_{qt}^{Q,E} - p_t^{E+} - \sum_{g \in \Omega^G} p_{gt}^{G,E} = 0 \quad (39)$$

$$v_t^{E+} - \lambda^E + \underline{\mu}^{E+} - \overline{\mu}^{E+} = 0 \quad (40)$$

$$-v_t^{E-} + \lambda^E - \underline{\mu}^{E-} + \overline{\mu}^{E-} = 0 \quad (41)$$

$$\alpha_{gt}^{G,E} - \lambda^E - \underline{\mu}_{gt}^{G,E} + \overline{\mu}_{gt}^{G,E} = 0 \forall g \in \Omega^G \tag{42}$$

$$-\alpha_{qt}^{Q,E} + \lambda^E - \underline{\mu}_{qt}^{Q,E} + \overline{\mu}_{qt}^{Q,E} = 0 \forall q \in \Omega^Q \tag{43}$$

$$0 \leq \underline{\mu}_{gt}^{G,E} \leq \underline{N}_{gt}^{G,E} \underline{u}_{gt}^{G,E}, \forall g \in \Omega^G \tag{44}$$

$$0 \leq \overline{\mu}_{gt}^{G,E} \leq \overline{M}_{gt}^{G,E} (1 - \underline{u}_{gt}^{G,E}), \forall g \in \Omega^G \tag{45}$$

$$0 \leq \underline{\mu}_{gt}^{G,E} \leq \overline{N}_{gt}^{G,E} \underline{u}_{gt}^{G,E}, \forall g \in \Omega^G \tag{46}$$

$$0 \leq \overline{\mu}_{gt}^{G,E} - \underline{p}_{gt}^{G,E} \leq \overline{M}_{gt}^{G,E} (1 - \underline{u}_{gt}^{G,E}), \forall g \in \Omega^G \tag{47}$$

$$0 \leq \underline{\mu}_{qt}^{Q,E} \leq \underline{N}_{qt}^{Q,E} \underline{u}_{qt}^{Q,E}, \forall q \in \Omega^Q \tag{48}$$

$$0 \leq \overline{\mu}_{qt}^{Q,E} \leq \overline{M}_{qt}^{Q,E} (1 - \underline{u}_{qt}^{Q,E}), \forall q \in \Omega^Q \tag{49}$$

$$0 \leq \underline{\mu}_{qt}^{Q,E} \leq \overline{N}_{qt}^{Q,E} \underline{u}_{qt}^{Q,E}, \forall q \in \Omega^Q \tag{50}$$

$$0 \leq \overline{\mu}_{qt}^{Q,E} - \underline{p}_{qt}^{Q,E} \leq \overline{M}_{qt}^{Q,E} (1 - \underline{u}_{qt}^{Q,E}), \forall q \in \Omega^Q \tag{51}$$

$$0 \leq \underline{\mu}_t^{E+} \leq \underline{N}_t^{E+} \underline{u}_t^{E+} \tag{52}$$

$$0 \leq \overline{\mu}_t^{E+} \leq \overline{M}_t^{E+} (1 - \underline{u}_t^{E+}) \tag{53}$$

$$0 \leq \underline{\mu}_t^{E+} \leq \overline{N}_t^{E+} \underline{u}_t^{E+} \tag{54}$$

$$0 \leq \overline{\mu}_t^{E+} - \underline{p}_t^{E+} \leq \overline{M}_t^{E+} (1 - \underline{u}_t^{E+}) \tag{55}$$

$$0 \leq \underline{\mu}_t^{E-} \leq \underline{N}_t^{E-} \underline{u}_t^{E-} \tag{56}$$

$$0 \leq \overline{\mu}_t^{E-} \leq \overline{M}_t^{E-} (1 - \underline{u}_t^{E-}) \tag{57}$$

$$0 \leq \underline{\mu}_t^{E-} \leq \overline{N}_t^{E-} \underline{u}_t^{E-} \tag{58}$$

$$0 \leq \overline{\mu}_t^{E-} - \underline{p}_t^{E-} \leq \overline{M}_t^{E-} (1 - \underline{u}_t^{E-}) \tag{59}$$

$$\underline{u}_{gt}^{G,E}, \overline{u}_{gt}^{G,E}, \underline{u}_{qt}^{Q,E}, \overline{u}_{qt}^{Q,E}, \underline{u}_t^{E+}, \overline{u}_t^{E+}, \underline{u}_t^{E-}, \overline{u}_t^{E-} \in \{0, 1\}, \forall g \in \Omega^G, \forall q \in \Omega^Q \tag{60}$$

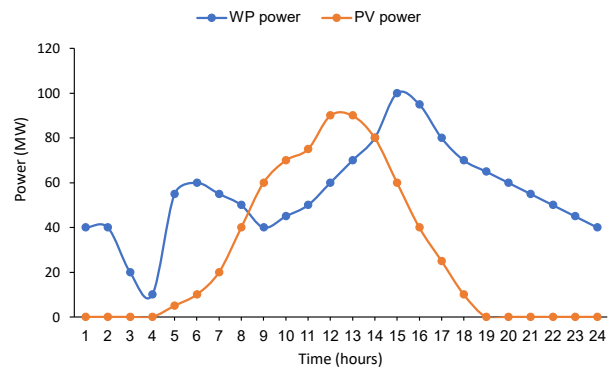


Fig. 3 The forecasted data of WP and PV

Table 2

BG generators' technical data

Generator	$P_i^B$ (MW)	$\overline{P}_i^B$ (MW)	$C^F$ (\$/MWh)	$C^V$ (\$/MWh)
1	0	30	4	3.7
2	0	40	6	3.7

The BG's power output depends on the amount of biogas stored in the storage converted into electric power (MWh). In literature, some studies consider the additional amount of biogas in the storage every hour as a constant. However, this paper assumes that biogas production can be adjusted flexibly, obtained by demand-oriented feeding. Reference (Mauky *et al.*, 2017) shows that demand-driven biogas production not only saves a significant amount of gas reserve required but also makes power generation much more flexible than continuous gas production. Fig. 3b illustrates the flow of gas over the 24-hour horizon. It can be seen that during the noon period, the additional amount of gas is not high, even zero in hours 10 and 11, because the PV power output is quite high during these hours. Note that increasing the VPP's power output can be more

### 3. Results and Discussion

#### 3.1 Study system

In this section, the proposed optimal model is applied to a CVPP test system including WPs, PVs, a BG with two generators, ESSs and local customers. The VPP operator determines the VPP's optimal scheduling based on the forecasted power output of WPs and PVs described in Fig. 3. Accordingly, the WPs' aggregated power output can reach 100MW at hour 15 while the PVs' highest available power is 90MW at hours 12 and 13. Besides, the ESSs are considered as a large-scale ESS with the technical data shown in Table 1. Similar, all local customers are aggregated as a single load with the forecasted consumption illustrated in Fig. 2a. The technical data of BG generators are presented in Table 2. The operating cost of WP and PV is assumed to be very small and can be ignored.

Table 1

ESS' technical data

$\overline{P}^{S,C}$ (MW)	$\overline{P}^{S,D}$ (MW)	$\eta^{S,C}$	$\eta^{S,D}$	$\overline{E}_t^S$ (MWh)	$e_0^S$ (MWh)
25	25	0.9	0.9	100	$0.5 \times \overline{E}_t^S$

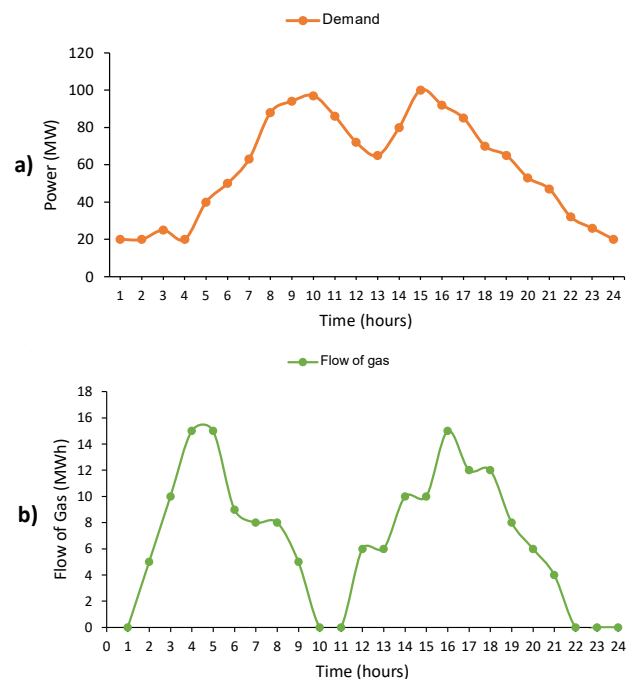


Fig. 2 Forecasted data of the VPP's demand and the flow of gas into the storage in each hour

**Table 3**  
Offer power and offer price of producers in some typical hours

	Block	Offer power (MW)			Offer price (\$/MWh)		
		t1	t10	t16	t1	t10	t16
GENCO 1	1	240	320	315	12	59	60
	2	50	100	100	14	61	62
	3	50	150	120	15	63	64
GENCO 2	1	300	420	420	42	58	57
	2	50	200	140	43	59	58
	3	50	200	100	45	61	60
GENCO 3	1	250	340	300	40	63	55
	2	70	140	120	42	65	57
	3	50	100	120	43	67	59
GENCO 4	1	180	260	230	10	51	47
	2	60	90	70	11	54	51
	3	30	90	50	13	57	53

profitable, but redundant power output will lead to a lower market-clearing price, thereby reducing the VPP's profit.

In addition to VPP, this paper assumes that four GENCOs and three retailers participate in the DA market. GENCOs have an offer curve consisting of three blocks of power quantities at different prices. Besides, GENCOs often proactively forecast the day-ahead electricity demand and give corresponding offer curves for each hour to increase profit opportunities. Table 3 presents the offer curves of each GENCO submitted to the DA market for some hours. It can be seen that at the peak-load hours, such as hour 10 and hour 16, each GENCO will offer more power at a higher offering price in comparison to the off-peak hour (hour 1). Similarly, each retailer submits a bid curve including three blocks of power quantities for each hour in the next operating day. The bid curves of retailers for some hours are shown in Table 4. The given data shows that the VPP's maximum production/consumption is quite high compared to the other GENCOs/retailers. So, the VPP test system can act as a price maker in the DA market.

The VPP optimal schedule in the DA market is determined by CPLEX version 12.6 (IBM, n.d.) under GAMS 40.3.0 environment (Richard, 2016) on a 64-bit core i5 1.9GHz personal computer with 16GB RAM. The impact of different aspects, such as ESS sizing or RES capacity, is also evaluated.

**Table 4**  
Bid power and bid price of retailers in some typical hours

	Block	Bid power (MW)			Bid price (\$/MWh)		
		t1	t10	t16	t1	t10	t16
Retailer 1	1	100	250	400	13	58	57
	2	300	225	150	12	56	56
	3	100	250	175	11	55	54
Retailer 2	1	100	425	500	20	59	56
	2	200	300	200	19	57.5	54.5
	3	300	150	250	17	55.5	53
Retailer 3	1	100	550	450	12	58	60
	2	100	200	350	10.5	57	59
	3	440	345	350	9.5	56	58

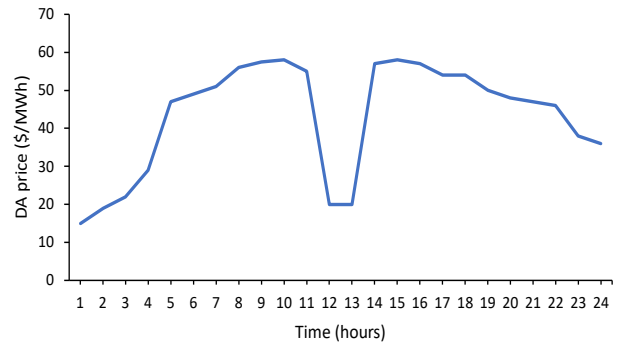


**Fig. 5** The DA market-clearing price

3.2 Numerical results

Based on forecast data of inner resources and demand as well as offer/bid information of other participants in the market, the VPP operator predicts the DA market price and determines its optimal offer/bid strategy to maximize its profit. The cleared market price is illustrated in Fig. 5. It can be seen that the market-clearing price is quite low at some hours; for example, the market-clearing prices in hours 1, 12, or 13 are equal or less than 20(\$/MWh). It can be explained that at these hours, the total demand of VPP and other retailers is low, and the offering power is redundant. By contrast, during peak-load hours, such as from hour 8 to hour 11, and hour 14 to hour 16, the power output of GENCOs is mobilized even in blocks of power quantities having high offer prices. As a result, the market price at these hours is significantly high – approximately 58(\$/MWh).

Fig. 4 shows the VPP's optimal schedule for each hour on the next operating day. The dashed line shows the VPP's trading strategy in the DA market, with a positive value representing the selling power and a negative value representing the purchasing power. Besides, the power output of WP and PV is described in Fig. 6, while Fig. 7a shows the operation of BG. As can be seen in Fig. 5 and Fig. 4, VPP will take advantage of its resources to sell energy at high-price hours, specifically from hour 8 to hour 11, and hour 14 to hour 16. In detail, Fig. 7a shows that BG's generators operate at maximum capacity during hours 8-11 and hours 14-16 because BG's operating cost of 3.7(\$/MWh) is significantly lower than the market-clearing price of 58(\$/MWh). Besides, the available power output of WP and PV

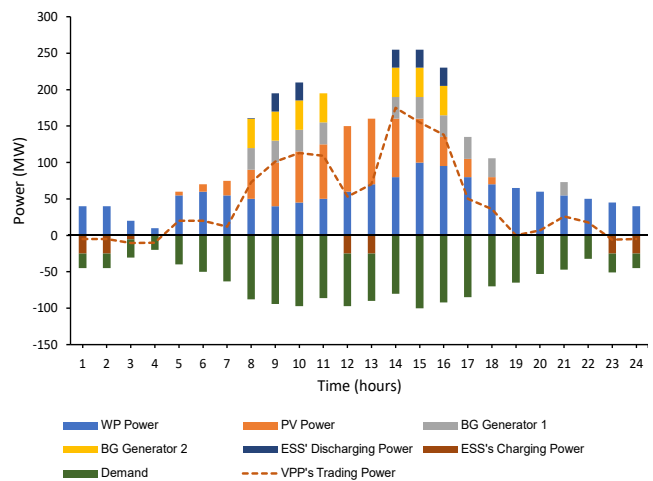


**Fig. 4** The VPP's optimal schedule in the DA market

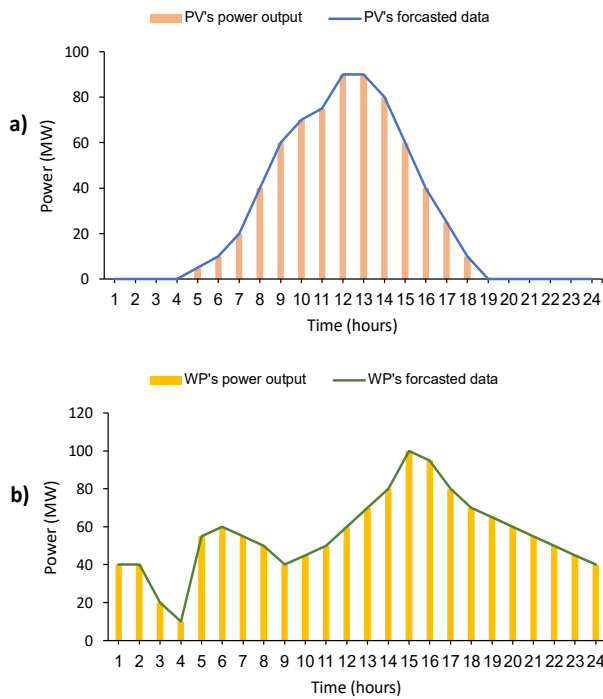


**Fig. 6** The operating schedule of PV and WP: a) PV's power production; b) WP's power production

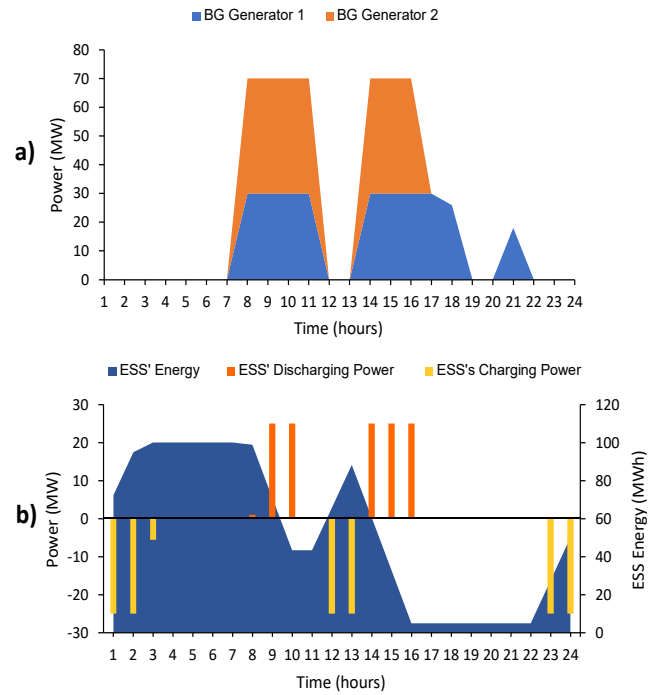


**Fig. 7** The operating data of BG and ESS: a) The BG's power production; b) The ESS' charging/discharging power

is fully utilized (Fig. 6). As a result, the VPP can achieve the highest profit.

On the other hand, during hours 1 to 4 and hours 23 and 24, the VPP should buy energy from the power network because PV and WP's power output is insufficient to supply the VPP's local customers (Fig. 4). It can be seen that VPP can operate BG to supply the local customers during these hours at the cost of only 3.7(\$/MWh) (Table 2), much lower than the market-clearing price of about 20(\$/MWh). However, buying electricity from the system during these periods and accumulating biogas to be able to operate BG at maximum capacity at high-price hours will help VPP gain more profit. Fig. 7a also clearly shows that BG only operates during hours with high market-clearing prices (hours 8-11, hours 14-16).

Fig. 7b shows the flexibility in the ESS operation. ESS will charge if the market-clearing price is low, for example, at midnight, with a market price of only 15(\$/MWh). Besides, ESS also charges when the available power output of VPP's inner resources is redundant, but the market price is not attractive enough, specifically at hours 12 and 13. By contrast, ESS discharge during periods of high market-clearing prices, such as from hours 14 to 16, with market-clearing prices of 58(\$/MWh); consequently, the VPP can obtain more revenue. The impacts of different parameters on the VPP's optimal operation are evaluated by the following sections:

### 3.2.1 Impact of the offering/bidding price of each producer/retailer in the DA market.

This section applies the optimal model to a new case study, named Case 1, to evaluate the impact of the offering/bidding price of other producers/retailers on the VPP's optimal scheduling. In this case, we increase the offering/bidding prices of the other producer/retailer during hours 1 to 4, hours 12 and 13, hours 23 and 24 while keeping the offering/bidding prices of the remaining hours the same. For example, in the original case study, the offering prices of GENCO 1 in hour 12

corresponding to three blocks of offering power are from 18, 20, and 22(\$/MWh). In Case 1, these prices increase to 55, 57, and 59(\$/MWh), respectively. Meanwhile, the other input parameters are similar to the original case study.

With the given above data, the obtained DA market-clearing price is presented in Fig. 9. It is easy to see that a higher offering/bidding price will cause the cleared market price to increase accordingly. For example, the market-clearing at hour 12 in the original case is 20(\$/MWh) (Fig. 5); after the GENCOs increase their offering price, the price at hour 12 becomes 52(\$/MWh) (Fig. 9). This is because VPP can only meet part of the needs of retailers, the rest is provided by GENCOs.

Note that VPP includes WP and PV with almost zero production costs. In addition, Table 2 shows that the fixed and variable costs of BG generators are 4, 6, and 3.7(\$/MWh), respectively - much lower than the offering price of GENCOs (Table 3). So, the offering price of VPP can be lower than any GENCO, and VPP can sell all excess power output to the system after supplying to local demand. Consequently, when comparing the results of the original case and Case 1 presented in Fig. 4 and Fig. 10, it can be seen that the selling/purchasing power of VPP changes very little. However, at hour 12 and hour 13, there is a significant difference in the DA cleared price of the original case and Case 1 leading to the change in the VPP's operating plan at these hours. In detail, the original case has the DA cleared price at hours 12 and 13 only 20(\$/MWh) so that a part of VPP's power output is stored in the ESS instead of being sold to the grid (Fig. 4). By contrast, this price in Case 1 is 52\$/MWh - much higher than in the original case - so VPP sells all excess energy to the system to obtain more revenue (Fig. 10).

### 3.2.2 The impact of ESS sizing

This section evaluates the effect of the ESS sizing on the VPP optimal operation. The proposed problem is performed with two scenarios of ESS sizing: Case 2 with ESS 10MW/100MWh and Case 3 with ESS 50MW/100MWh while the other input

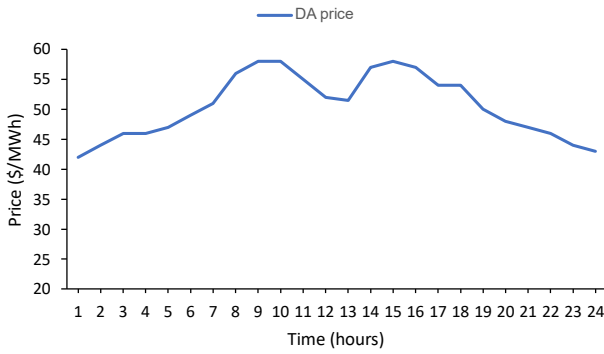


**Fig. 9** Case 1: The DA market-clearing price in case the offering/bidding of each producer/retailer increase

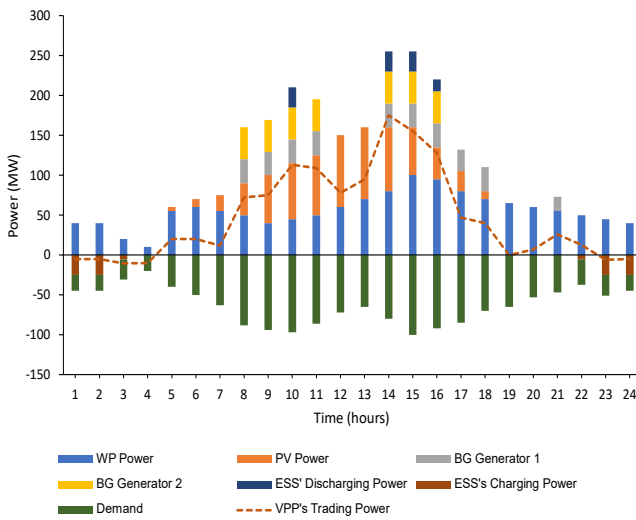


**Fig. 10** Case 1: The VPP's optimal schedule in the DA market in case the offering/bidding of each producer/retailer increase

data are kept unchanged. The VPP's optimal trading power and the ESS' optimal operation in these cases are respectively presented in Fig. 8 and Fig. 11 and compared with the original case study in Fig. 4 and Fig. 7b. It can be seen that the ESS' discharging power can be a part of VPP's selling power. Therefore, when the ESS's rated power increases from 10MW to 50MW, the VPP's selling power in some hours also increases. Based on VPP's operating plan optimization model in Section 2, the ESS' discharging power mainly increases at the hours of high market-clearing price, such as hours 14. Fig. 7b shows that in the original case, ESS discharges with a rated power of 25MW at hour 14. Similarly, in Case 2, ESS discharges with the rated power of 10MW, while in Case 3, the ESS' discharging power is 31MW at this period. Consequently, the VPP's selling power at hour 14 increases from 160MW to 175 and 180 MW when the ESS' rated power increases from 10 to 25 and 50MW, respectively (Fig. 4, Fig. 8a, Fig. 11a). As a result, the VPP can obtain more revenue. Fig. 12 shows that VPP's profit is approximately 46000\$ in the case of ESS 10MW/100MWh while VPP can obtain about 50000\$ if ESS sizing is 50MW/100MWh.

Besides, Fig. 8b and Fig. 11b show that ESS can only contribute to the VPP's selling power for a few hours due to the limitation of ESS capacity. In detail, with the ESS' capacity of 100MWh, an increase in the ESS' rated power from 10MW to 50MW will reduce the charging/discharging time from 10 hours to 2 hours. Consequently, the number of hours that ESS can participate in VPP's selling power decreases. While ESS

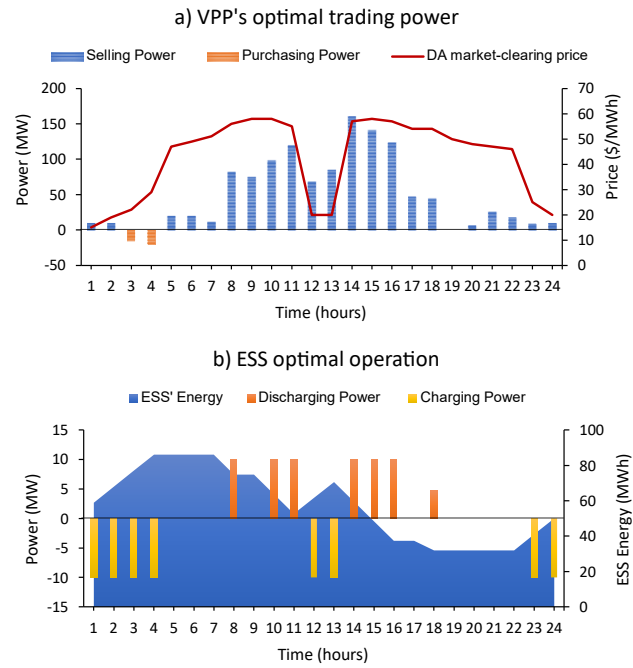


**Fig. 8** Case 2: The VPP's optimal trading power and the ESS' optimal operation with ESS sizing of 10MW/100MWh

10MW/100MWh can discharge continuously from hour 14 to hour 16 and hour 18, ESS 50MW/100MWh can only provide energy during hours 14 and 15. However, blue areas in Fig. 8b and Fig. 11b show that the proposed optimization model always keeps the ESS having enough energy to discharge during the hours of the high market price (hours 9-10, hours 14-15). In addition, it is exciting that the market price in these scenarios is almost unchanged. This can be explained by the fact that ESS only contributes a small part of VPP's trading power.

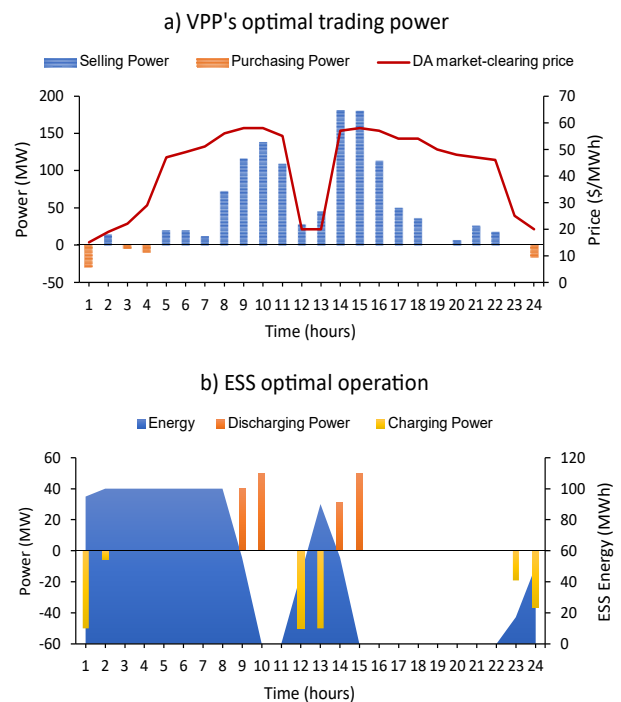


**Fig. 11** Case 3: The VPP's optimal trading power and the ESS' optimal operation with ESS sizing of 50MW/100MWh



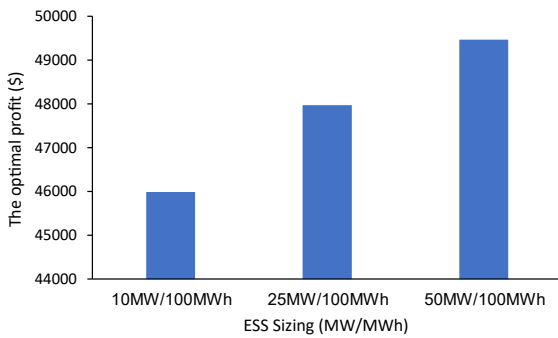


Fig. 12 The VPP's optimal profit depending on the ESS sizing

4. Conclusion

This paper considers and analyzes the optimal trading strategy of a VPP that acts as a price-maker participant in the DA market. The main purpose is predetermining the DA market-clearing price based on the information collected about the offering/bidding quantity and price of the other producers and retailers, then calculating the VPP's optimal selling/purchasing power at each hour on the next operating day. In addition, the optimal cooperation between the VPP's inner resources, ESS, and customers are also determined to obtain the highest profit. To solve this problem, we build a bi-level optimization model with the upper-level model maximizing the VPP's profit, and the lower-level model is the DA market clearing problem. The cleared price and the VPP's optimal scheduling are obtained. The influence of each agent's offering/bidding price and ESS sizing on the results is studied and analyzed.

The results show that due to low operating costs, VPP can offer excess capacity at a price equal to or lower than the anticipated market price. Therefore, all excess capacity of VPP is accepted to be sold to the power system. For the same reason, the offer/bid prices of other participants influence the market's clear price but have almost no impact on the trading scenario of VPP. Meanwhile, the size of ESS affects VPP's buying/selling capacity and thereby affects VPP's profit.

The proposed model can be applied to any VPP model regardless of the type of RESs or local load. Moreover, this model can also be adapted to study the effect of uncertainty in RES and loads. These other resources or demands, such as the demand response or electric vehicle charging station, can also be considered in the VPP. These topics are left to future works.

Nomenclature

A. Indexes and Sets

- $d$  Demands in the VPP.
- $g \in \Omega^G$  The other producers in the DA market.
- $q \in \Omega^Q$  The other retailers in the DA market.
- $t \in \Omega^T$  Time intervals.
- $i \in \Omega^I$  Generators of BG inside VPP.

B. Parameters

- $C^{BG}$  The BG's operating cost [\\$]
- $C_i^F$  The fixed cost of the BG's generator  $i$  [\$/MW]
- $C_i^V$  The variable cost of the BG's generator  $i$  [\$/MW]
- $c^{WD}$  The operating cost of WP [\$/MW]
- $C^{WD}$  The total operating cost of WP [\\$]
- $E^S$  The ESS' minimum energy level [MWh].
- $\bar{E}^S$  The ESS' rated capacity [MWh].
- $\eta^S$  The ESS' charging/discharging efficiency [%].

- $F_t$  The flow of gas (expressed in MWh) into the BG's storage in hour  $t$  [MWh].
- $\bar{P}_i^B$  Maximum power output of the BG's generator  $i$  [MW].
- $\underline{P}_i^B$  Minimum power output of the BG's generator  $i$  [MW].
- $\overline{SOC}^B$  The rated capacity of gas storage inside BG [MWh].
- $\bar{P}_t^{WD}$  The WP's forecasted power output at time  $t$  [MW].
- $\bar{P}_t^{PV}$  The PV's forecasted power output at time  $t$  [MW].
- $\bar{P}^S$  The ESS' rated power [MW].
- $P_{d,t}^{VPP}$  The forecasted consumption of local customers in VPP at time  $t$  [MW].
- $\bar{P}_{gt}^{G,E}$  The offer quantity of producer  $g$  in the DA market at time  $t$  [MW].
- $\bar{P}_{qt}^{Q,E}$  The bid quantity of retailer  $q$  in the DA market at time  $t$  [MW].
- $\alpha_{gt}^{G,E}$  Offer price of producer  $g$  in the DA market at time  $t$  [\$/MWh].
- $\alpha_{qt}^{Q,E}$  Bid price of retailer  $q$  in the DA market at time  $t$  [\$/MWh].

C. Variables

- $p_t^{WD}$  The WP's power output at time  $t$  [MW].
- $p_t^{PV}$  The PV's power output at time  $t$  [MW].
- $u_t^{PV}$  Binary variable shows the PV's operating situation at time  $t$
- $\bar{P}_{it}^B$  The power output of the BG's generator  $i$  at time  $t$  [MW].
- $soc_t^B$  The energy stored in the BG's gas storage at time  $t$  [MWh].
- $u_{it}^B$  Binary variable shows the operating situation of the BG's generator  $i$  at time  $t$ .
- $p_t^{S,C}$  The ESS' charging power at time  $t$  [MW].
- $p_t^{S,D}$  The ESS' discharging power at time  $t$  [MW].
- $e_t^S$  The ESS' energy at time  $t$  [MWh].
- $u_t^S$  Binary variable shows the ESS' charging/discharging state at time  $t$ .
- $p_t^{E+}$  The VPP's selling power in the DA market at time  $t$  [MW].
- $p_t^{E-}$  The VPP's purchasing power in the DA market at time  $t$  [MW].
- $\bar{P}_t^{E+}$  The VPP's offer quantity submitted to the DA market at time  $t$  [MW].
- $\bar{P}_t^{E-}$  The VPP's bid quantity submitted to the DA market at time  $t$  [MW].
- $v_t^{E+}$  The VPP's offer price submitted to the DA market at time  $t$  [\$/MWh].
- $v_t^{E-}$  The VPP's bid price submitted to the DA market at time  $t$  [\$/MWh].
- $u_t^{VPP}$  Binary variable shows VPP's selling/purchasing situation.
- $\lambda_t^E$  The DA market-clearing price at time  $t$  [\$/MWh].

**Author Contributions:** Conceptualization, methodology, formal analysis, supervision, writing—review and editing, Nguyen Hong Nhung; formal analysis, software, writing—original draft, Bui Quang Khai; data curation, writing—original draft project, Phan Vo Thanh Long; data curation, writing—original draft, Bui Huynh Duc. All authors have read and agreed to the published version of the manuscript.

**Funding:** This research is funded by the Ministry of Education and Training, Vietnam under the grant number CT2022.07.BKA.05.

**Conflicts of Interest:** The authors declare no conflict of interest

References

AEMO. (2021). AEMO NEM Virtual Power Plant Demonstrations. <https://aemo.com.au/-/media/files/initiatives/der/2021/vpp-demonstrations-knowledge-sharing-report-4>

ARENA. (2021). South Australia Virtual Power Plant Phase 3A. <https://arena.gov.au/assets/2021/08/tesla-virtual-power-plant-lessons-learn-1.pdf>

Baringo, A., & Baringo, L. (2017). A Stochastic Adaptive Robust Optimization Approach for the Offering Strategy of a Virtual Power Plant. *IEEE Transactions on Power Systems*, 32(5), 3492–3504. <https://doi.org/10.1109/TPWRS.2016.2633546>

- Baringo, A., Baringo, L., & Arroyo, J. M. (2019). Day-Ahead Self-Scheduling of a Virtual Power Plant in Energy and Reserve Electricity Markets under Uncertainty. *IEEE Transactions on Power Systems*, 34(3), 1881–1894. <https://doi.org/10.1109/TPWRS.2018.2883753>
- Baringo, L., Freire, M., Garcia-Bertrand, R., & Rahimiyan, M. (2021). Offering strategy of a price-maker virtual power plant in energy and reserve markets. *Sustainable Energy, Grids and Networks*, 28, 100558. <https://doi.org/10.1016/J.SEGAN.2021.100558>
- British Chamber of Commerce Vietnam. (2022). Vietnam Renewable Energy Report. <https://britchamvn.com/wp-content/uploads/2022/04/156e6152-729f-4225-89b9-ff1ad516b803.pdf>
- Das, K. (2020). Renewables in Vietnam: Current Opportunities and Future Outlook. Vietnam Briefing. <https://www.vietnam-briefing.com/news/vietnams-push-for-renewable-energy.html/>
- Ding, H., Pinson, P., Hu, Z., Wang, J., & Song, Y. (2017). Optimal Offering and Operating Strategy for a Large Wind-Storage System as a Price Maker. *IEEE Transactions on Power Systems*, 32(6), 4904–4913. <https://doi.org/10.1109/TPWRS.2017.2681720>
- Electricity Regulatory Authority of Vietnam. (2018, September 27). Circular: Regulations on operation of the competitive electricity generation market. [http://www.erav.vn/userfile/User/trungnla/files/2020/10/TT\\_28\\_2018\\_TT\\_BCT.pdf](http://www.erav.vn/userfile/User/trungnla/files/2020/10/TT_28_2018_TT_BCT.pdf)
- Fernández-Muñoz, D., & Pérez-Díaz, J. I. (2023). Optimisation models for the day-ahead energy and reserve self-scheduling of a hybrid wind–battery virtual power plant. *Journal of Energy Storage*, 57. <https://doi.org/10.1016/J.EST.2022.106296>
- Gazijahani, F. S., & Salehi, J. (2020). IGDT-Based Complementarity Approach for Dealing with Strategic Decision Making of Price-Maker VPP Considering Demand Flexibility. *IEEE Transactions on Industrial Informatics*, 16(4), 2212–2220. <https://doi.org/10.1109/TII.2019.2932107>
- Helman, U. (2019). Distributed energy resources in the US wholesale markets: Recent trends, new models, and forecasts. In Consumer, Prosumer, Prosumer: How Service Innovations will Disrupt the Utility Business Model (1st ed., pp. 431–469). Academic Press/Elsevier. <https://doi.org/10.1016/B978-0-12-816835-6.00019-X>
- Hu, J., Jiang, C., & Liu, Y. (2019). Short-Term Bidding Strategy for a Price-Maker Virtual Power Plant Based on Interval Optimization. *Energies*, 12(19), 3662. <https://doi.org/10.3390/EN12193662>
- IBM. (n.d.). ILOG CPLEX Optimization Studio | IBM. Retrieved March 31, 2022, from <https://www.ibm.com/products/ilog-cplex-optimization-studio>
- Internationale Klimaschutzinitiative. (2022, December 12). Vietnam: Biogas plants to reduce greenhouse gas emissions | Internationale Klimaschutzinitiative (IKI). <https://www.international-climate-initiative.com/en/iki-media/news/vietnam-biogas-plants-to-reduce-greenhouse-gas-emissions/>
- Kardakos, E. G., Simoglou, C. K., & Bakirtzis, A. G. (2016). Optimal Offering Strategy of a Virtual Power Plant: A Stochastic Bi-Level Approach. *IEEE Transactions on Smart Grid*, 7(2), 794–806. <https://doi.org/10.1109/TSG.2015.2419714>
- Kieny, C., Bersenneff, B., Hadjsaid, N., Besanger, Y., & Maire, J. (2009). On the concept and the interest of Virtual Power plant: Some results from the European project FENIX. 2009 *IEEE Power and Energy Society General Meeting, PES '09*. <https://doi.org/10.1109/PES.2009.5275526>
- Kuiper, G. (2022). What Is the State of Virtual Power Plants in Australia? From Thin Margins to a Future of VPP-tailers (Issue March). [https://ieefa.org/wp-content/uploads/2022/03/What-Is-the-State-of-Virtual-Power-Plants-in-Australia\\_March-2022\\_2.pdf](https://ieefa.org/wp-content/uploads/2022/03/What-Is-the-State-of-Virtual-Power-Plants-in-Australia_March-2022_2.pdf)
- Lee, J., & Won, D. (2021). Optimal Operation Strategy of Virtual Power Plant Considering Real-Time Dispatch Uncertainty of Distributed Energy Resource Aggregation. *IEEE Access*, 9, 56965–56983. <https://doi.org/10.1109/ACCESS.2021.3072550>
- Mashhour, E., & Moghaddas-Tafreshi, S. M. (2011). Bidding strategy of virtual power plant for participating in energy and spinning reserve markets-Part I: Problem formulation. *IEEE Transactions on Power Systems*, 26(2), 949–956. <https://doi.org/10.1109/TPWRS.2010.2070884>
- Mauky, E., Weinrich, S., Jacobi, H. F., Nägele, H. J., Liebetrau, J., & Nelles, M. (2017). Demand-driven biogas production by flexible feeding in full-scale – Process stability and flexibility potentials. *Anaerobe*, 46, 86–95. <https://doi.org/10.1016/J.ANAEROBE.2017.03.010>
- Neme, C., Energy Futures Group, Cowart, R., & Regulator Assistance Project. (2014). Energy Efficiency Participation in Electricity Capacity Markets – The US Experience. <https://www.raponline.org/knowledge-center/energy-efficiency-participation-in-electricity-capacity-markets-the-us-experience/>
- Next-Kraftwerke. (n.d.). Virtual Power Plant: The Power of Many. Retrieved April 19, 2023, from <https://www.next-kraftwerke.com/vpp>
- Ngo, C. (2021, October 27). Can solar power be curtailed by about 8 billion kWh in 2021? <https://laodong.vn/kinh-doanh/dien-mat-troi-co-the-bi-cat-giam-khoang-8-ti-kwh-trong-nam-2021-9612451do>
- Nguyen-Duc, H., & Nguyen-Hong, N. (2020). A study on the bidding strategy of the Virtual Power Plant in energy and reserve market. *Energy Reports*, 6, 622–626. <https://doi.org/10.1016/J.EGYR.2019.11.129>
- Nguyen, H. T., Le, L. B., & Wang, Z. (2018). A Bidding Strategy for Virtual Power Plants with the Intraday Demand Response Exchange Market Using the Stochastic Programming. *IEEE Transactions on Industry Applications*, 54(4), 3044–3055. <https://doi.org/10.1109/TIA.2018.2828379>
- Noi, S., Jelinek, M., & Roubik, H. (2022). Small-scale biogas plants in Vietnam: How are affected by policy issues? *Ecological Questions*, 33(4), 1–38. <https://doi.org/10.12775/EQ.2022.037>
- Oureilidis, K., Malamaki, K. N., Gallos, K., Tsimmelis, A., Dikaiakos, C., Gkavanoudis, S., Cvetkovic, M., Mauricio, J. M., Ortega, J. M. M., Ramos, J. L. M., Papaioannou, G., & Demoulias, C. (2020). Ancillary services market design in distribution networks: Review and identification of barriers. *Energies*, 13(4). <https://doi.org/10.3390/en13040917>
- Pal, P., Krishnamoorthy, P. A., Rukmani, D. K., Antony, S. J., Ocheme, S., Subramanian, U., Elavarasan, R. M., Das, N., & Hasanien, H. M. (2021). Optimal Dispatch Strategy of Virtual Power Plant for Day-Ahead Market Framework. *Applied Sciences* 11(9), 3814. <https://doi.org/10.3390/APP11093814>
- Pudjianto, D., Ramsay, C., & Strbac, G. (2007). Virtual power plant and system integration of distributed energy resources. *IET Renewable Power Generation*, 1(1), 10–16. <https://doi.org/10.1049/iet-rpg:20060023>
- Renewable Energy Agency, I. (2012). RENEWABLE ENERGY TECHNOLOGIES: COST ANALYSIS SERIES Biomass for Power Generation Acknowledgement. <https://www.irena.org/publications/2012/Jun/Renewable-Energy-Cost-Analysis--Biomass-for-Power-Generation>
- Richard, E. R. (2016). GAMS: A User's Guide. GAMS Development Corporation.
- Steven A. Gabriel, Antonio J. Conejo, J. David Fuller, Benjamin F. Hobbs, Carlos Ruiz, Gabriel, S. A., Conejo, A. J., Fuller, J. D., Hobbs, B. F., & Ruiz, C. (2013). Complementarity Modeling in Energy Markets. In Springer (Vol. 180). <https://doi.org/10.1007/978-1-4419-6123-5>
- Tavakoli, A., Karimi, A., & Shafie-Khah, M. (2021). Linearized Stochastic Optimization Framework for Day-Ahead Scheduling of a Biogas-Based Energy Hub under Uncertainty. *IEEE Access*, 9, 136045–136059. <https://doi.org/10.1109/ACCESS.2021.3116028>
- Vahedipour-Dahraie, M., Rashidizadeh-Kermani, H., Shafie-Khah, M., & Catalão, J. P. S. (2021). Risk-Averse Optimal Energy and Reserve Scheduling for Virtual Power Plants Incorporating Demand Response Programs. *IEEE Transactions on Smart Grid*, 12(2), 1405–1415. <https://doi.org/10.1109/TSG.2020.3026971>
- Yang, H., Li, C., Huang, R., Wang, F., Hao, L., Wu, Q., & Zhou, L. (2023). Bi-level Energy Trading Model Incorporating Large-scale Biogas Plant and Demand Response Aggregator. *Journal of Modern Power Systems and Clean Energy*, 11(2), 567–578. <https://doi.org/10.35833/MPCE.2021.000632>
- Yazdaninejad, M., Amjady, N., & Dehghan, S. (2020). VPP Self-Scheduling Strategy Using Multi-Horizon IGDT, Enhanced Normalized Normal Constraint, and Bi-Directional Decision-

- Making Approach. *IEEE Transactions on Smart Grid*, 11(4), 3632–3645. <https://doi.org/10.1109/TSG.2019.2962968>
- Yi, Z., Xu, Y., Wang, H., & Sang, L. (2021). Coordinated Operation Strategy for a Virtual Power Plant with Multiple DER Aggregators. *IEEE Transactions on Sustainable Energy*, 12(4), 2445–2458. <https://doi.org/10.1109/TSTE.2021.3100088>
- Zhao, Q., Shen, Y., & Li, M. (2016). Control and Bidding Strategy for Virtual Power Plants with Renewable Generation and Inelastic Demand in Electricity Markets. *IEEE Transactions on Sustainable Energy*, 7(2), 562–575. <https://doi.org/10.1109/TSTE.2015.2504561>
- Zhou, Y., Wei, Z., Sun, G., Cheung, K. W., Zang, H., & Chen, S. (2019). Four-level robust model for a virtual power plant in energy and reserve markets. *IET Generation, Transmission and Distribution*, 13(11), 2006–2014. <https://doi.org/10.1049/iet-gtd.2018.5197>



© 2023. The Author(s). This article is an open access article distributed under the terms and conditions of the Creative Commons Attribution-ShareAlike 4.0 (CC BY-SA) International License (<http://creativecommons.org/licenses/by-sa/4.0/>)

**APPENDIX**

*A. Converting the MPEC model to the MILP model*

*A.1. Reformulating a bi-level MPEC problem into a single-level problem*

To reformulate a bi-level MPEC problem into a single-level problem, the lower-level problem, i.e., the DA market-clearing problem, is replaced by a Karush-Kuhn-Tucker (KKT) conditions as follows:

$$L(p_t^{E+}, p_{gt}^{G,E}, p_t^{E-}, p_{qt}^{Q,E}, \lambda_t^E, \underline{\mu}_{gt}^{G,E}, \underline{\mu}_{qt}^{Q,E}, \overline{\mu}_{gt}^{G,E}, \overline{\mu}_{qt}^{Q,E}, \underline{\mu}^{E+}, \overline{\mu}^{E+}, \underline{\mu}^{E-}, \overline{\mu}^{E-})$$

$$= v_t^{E+} p_t^{E+} + \sum_{g \in \Omega^G} \alpha_{gt}^{G,E} p_{gt}^{G,E} - v_t^{E-} p_t^{E-} - \sum_{q \in \Omega^Q} \alpha_{qt}^{Q,E} p_{qt}^{Q,E} + \lambda_t^E (p_t^{E-} + \sum_{q \in \Omega^Q} p_{qt}^{Q,E} - p_t^{E+} - \sum_{g \in \Omega^G} p_{gt}^{G,E}) + \underline{\mu}_{gt}^{G,E} (-p_{gt}^{G,E}) + \overline{\mu}_{gt}^{G,E} (p_{gt}^{G,E} - \overline{p}_{gt}^{G,E}) + \underline{\mu}_{qt}^{Q,E} (-p_{qt}^{Q,E}) + \overline{\mu}_{qt}^{Q,E} (p_{qt}^{Q,E} - \overline{p}_{qt}^{Q,E}) + \underline{\mu}^{E+} (-p_t^{E+}) + \overline{\mu}^{E+} (p_t^{E+} - \overline{p}_t^{E+}) + \underline{\mu}^{E-} (-p_t^{E-}) + \overline{\mu}^{E-} (p_t^{E-} - \overline{p}_t^{E-})$$
(61)

Find the partial derivative of L concerning the variable  $p_t^{E+}, p_t^{E-}, p_{gt}^{G,E}, p_{qt}^{Q,E}$ , the equations (40)-(43) are obtained.

From equations (18)-(21), we have the following complementary slackness conditions:

$$0 \leq \underline{\mu}^{E+} \perp p_t^{E+} \geq 0$$
(62)

$$0 \leq \overline{\mu}^{E+} \perp \overline{p}_t^{E+} - p_t^{E+} \geq 0$$
(63)

$$0 \leq \underline{\mu}^{E-} \perp p_t^{E-} \geq 0$$
(64)

$$0 \leq \overline{\mu}^{E-} \perp \overline{p}_t^{E-} - p_t^{E-} \geq 0$$
(65)

$$0 \leq \underline{\mu}_{gt}^{G,E} \perp p_{gt}^{G,E} \geq 0, \forall g \in \Omega^G$$
(66)

$$0 \leq \overline{\mu}_{gt}^{G,E} \perp \overline{p}_{gt}^{G,E} - p_{gt}^{G,E} \geq 0, \forall g \in \Omega^G$$
(67)

$$0 \leq \underline{\mu}_{qt}^{Q,E} \perp p_{qt}^{Q,E} \geq 0, \forall q \in \Omega^Q$$
(68)

$$0 \leq \overline{\mu}_{qt}^{Q,E} \perp \overline{p}_{qt}^{Q,E} - p_{qt}^{Q,E} \geq 0, \forall q \in \Omega^Q$$
(69)

*A.2. MILP model*

The single-level MPEC problem is a nonlinear single-level problem because it has these nonlinear functions:

- $\lambda_t^E (p_t^{E+} \Delta t - p_t^{E-} \Delta t)$  in the objective function (1)
- Constraints (62)-(69).

Therefore, these functions must be reformulate into linear form to apply MILP

*A.2.1. Linearization of  $\lambda_t^E (p_t^{E+} \Delta t - p_t^{E-} \Delta t)$*

Nonlinear function  $\lambda_t^E (p_t^{E+} \Delta t - p_t^{E-} \Delta t)$  is reformulated into a linear problem by the approach presented in (Steven A. Gabriel et al., 2013) as follows:

$$\lambda_t^E p_t^{E+} - \lambda_t^E p_t^{E-} = \sum_{q \in \Omega^Q} \alpha_{qt}^{Q,E} p_{qt}^{Q,E} - \sum_{g \in \Omega^G} \overline{p}_{gt}^{G,E} \overline{\mu}_{gt}^{G,E} - \sum_{g \in \Omega^G} \alpha_{gt}^{G,E} p_{gt}^{G,E} - \sum_{q \in \Omega^Q} \overline{p}_{qt}^{Q,E} \overline{\mu}_{qt}^{Q,E}$$
(70)

Replacing the term  $\lambda_t^E (p_t^{E+} \Delta t - p_t^{E-} \Delta t)$  in the objective function (1) by the righ-hand side of equation (70), we have the objective function (22) of a MILP model.

*A.2.2. Linearization of the complementary slackness conditions*

The nonlinear terms in the additional constraints have the form  $x \cdot y = 0$ , and  $x, y \geq 0$ . These nonlinear constraints can be reformulated by the following MILP equations:

$$0 \leq x \leq Mu$$
(71)

$$0 \leq y \leq M(1 - u)$$
(72)

$$u \in \{0,1\}$$
(73)

where M is a large-enough positive constant.

Consequently, constraints (62)-(69) can be reformulated by the equations (44)-(60).